8th World Conference on Experimental Heat Transfer, Fluid Mechanics, and Thermodynamics
June 16-20, 2013, Lisbon, Portugal

POOL BOILING HEAT TRANSFER OVER MICRO-PATTERNED SURFACES: EXPERIMENTS AND THEORY

E.Teodori, A. S. Moita* and A.L.N Moreira*

* IN+, Instituto Superior Técnico, Universidade Técnica de Lisboa, Av. Rovisco Pais, 1049-001 Lisbon, Portugal
E-mail (corresponding author): anamoita@dem.ist.utl.pt

***Keywords**: Pool boiling heat transfer, micro-patterned surfaces, thermophysical properties, PIV, bubble dynamics modeling*

1. INTRODUCTION

The use of modified surfaces (by coating and/or micro-and-nano-structuring) to enhance pool boiling heat transfer has been explored for many applications (e.g. [1, 2]). Most of these studies, including the aforementioned focus on increasing the Critical Heat Flux, by a trial and error approach, but quantification of the influence of surface topography and wettability on the heat transfer and on the induced flow regime are not yet successfully performed. The use of such approach is justified through the search of an optimal configuration for a specific application. However, this may not be the most effective approach given the lack of universality of the empirical correlations devised by this approach, as recently shown by McHale and Garimella [3]. These authors have also stressed the importance of understanding the effect of the surface topography in the bubble nucleation characteristics. Moita *et al*. [4] have explored in detail the effect of surface topography and of the liquid properties on bubble dynamics and suggested a relation linking the distance between micro-cavities and the heat transfer coefficient. Basically, one can determine an optimum distance which maximizes the heat transfer coefficient *h* by triggering bubble growth. Further decreasing that distance, bubble coalescence near the surface will be excessively strong causing a steep deterioration of *h*. The work performed in [4] produced guiding results, which should be confirmed for a wider range of refrigerants. Also, given the considerably high latent heat of evaporation of the liquids used in [4], the relations devised are mostly related to the heat transfer parcel associated to the latent heat. However, there are other two parcels involved in the pool boiling heat transfer, namely the natural convection and the bulk convection (induced by bubble growth and motion) [5] whose relative importance is not clearly accessed.

In line with this, the present work proceeds with the analysis suggested in [4] over a wider range of liquids to infer on the relative importance of the various pool boiling heat transfer parcels, when the latent heat is not the dominant one. The experimental approach combines heat transfer measurements, high speed visualization and PIV to infer on the effect of surface micro-structuring in the various heat transfer parcels. A detailed study relating bubble dynamics and the heat transfer parcels is now presented, as a work in progress of [4]. The PIV provides particularly interesting information on the bubbles vertical velocity, allowing to infer on the way the micro-structuring is affecting the bulk induced flow. Additionally, a theoretical analysis is performed to evaluate the three heat transfer parcels, including their influencing parameters. This analysis consists on the first mark of a step-by-step approach in the development of a simulation tool to infer on the efficiency and feasibility, from the thermodynamics point of view, of a practical system for cooling applications, based on the geometry used here.

2. EXPERIMENTAL PROCEDURE

The pool boiling is investigated for various liquids, namely the dielectric fluid HFE 7000, ethanol and water, to account for the liquid properties as well as to infer on the additional effects of wettability in the observed phenomena. The most relevant thermophysical properties of the working fluids are summarized in Table 1.

Table 1 Thermophysical properties of the liquids used in the present study, taken at saturation, at 1.013×10^5Pa.

Property	Ethanol	Water	HFE7000
T_{sat} [°C]	78.4	100	34
ρ_l [kg/m^3]	736.4	957.8	1374.7
ρ_v [kg/m^3]	1.647	0.5956	4.01
μ_l [mN m/s^2]	0.448	0.279	0.3437
C_{pl} [J/kgK]	3185	4217	1352.5
k_l [W/mK]	0.165	0.68	0.07
h_{fg} [kJ/kg]	849.9	2257	142
σ_{lv} [N/m]x10^3	17	58	12.4

Heat flux and heat transfer coefficients are determined for the various liquid/surface pairs. Afterwards, they are related to the bubble dynamics. This characterization is made by combining high-speed visualization with PIV measurements.

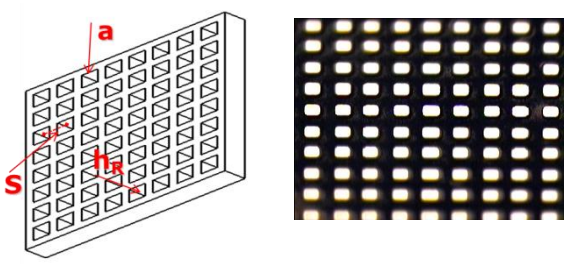

a) **b)**

Figure 1 **a)** Identification of the main parameters quantifying the micro-patterns. **b)** Sample of a pattern with square cavities.

The micro-cavities are squares with fized size length a and fixed depth h_R cross section with side length a=20 μm and depth h_R=20μm (see Figure 1). The distance between the centers of the cavities S is mainly our optimization variable, ranging between

300μm<*S*<1200μm. The parameters characterizing the micro-patterns are schematically defined in Figure 1, together with a photo of a sample.

The patterns are custom made from silicon wafers combining wet etching with plasma etching and the roughness profiles measured using a profile meter with a precision of ±100Angstroms. Table 2 depicts the main topographical characteristics of the surfaces used in this study. The Table includes the average values of the static contact angle, which were measured as described in [6]. The contact angles obtained with ethanol and HFE in contact with all the surfaces are close to zero.

Table 2 Main range of the topographical characteristics of the micro-patterned surfaces. θ is the average static contact angle measured with water at room temperature. θ≅0º for all the surfaces in contact with ethanol and HFE7000.

Material	**Reference**	a [μm]	h_R [μm]	S [μm]	θ [º]
Silicon Wafer	Smooth	≈ 0	≈ 0	≈ 0	86.0
	C1	52	20	304	90.0
	C2	52	20	400	91.5
	C3	52	20	464	71.5
	C4	52	20	626	86.5
	C5	52	20	700	95.0
	C6	52	20	800	60.5
	C7	52	20	1200	66.3

2.1 Heat transfer measurements

The boiling curves are presented for each liquid and each heating surface by varying the imposed heat flux in steps of 15W/cm^2. Each curve is obtained from the average of seven experiments. The liquid is degassed before each experiment by maintaining it in the pool at 20°C above the saturation temperature and the experimental procedure is started, for each heat flux, only after the system has reached thermal equilibrium, i.e. when the temperature oscillation is smaller than ±0.5 °C.

Experiments are conducted to obtain average boiling curves by both increasing and decreasing the heat flux, to infer on hysteresis effects, as also pointed by Mohamed and Bostanci [7]. The temperature measurements have an uncertainty of ±1°C. The relative error associated with the determination of the heat transfer is 5%.

2.2 Image analysis of bubble dynamics

Following an approach similar to that presented in many works reported in the literature, the bubble nucleation parameters selected in the present study are the bubble departure diameter, the bubble departure frequency and the active nucleation sites density. This characterization is based on high-speed visualization and image post-processing. The images are recorded with a frame rate of 2200fps. For the optical configuration used here, the spatial resolution is 9.346μm/pixel.

The bubble departure diameter is measured for each test condition from 300 to 1060 frames. For each image a mean value is averaged from 5-16 measurements for every nucleation site that is identified in the frame.

At higher heat fluxes, the various interaction mechanisms, which will be discussed in the following section, may alter significantly the value of the departure diameter, especially when horizontal coalescence occurs. Therefore, in those cases, the measured diameters are a mean value taken from the averaged diameters, which are evaluated after the occurrence of such events close to the wall.

The error associated to the measurements of the bubble departure diameter is ±9.346 μm.

The bubble departure frequency is estimated by determining the time elapsed between apparent departure events, which are counted for a defined interval of time. The departure frequency is assessed, for each test condition, for at least five nucleation sites, which are evaluated based on extensive image post-processing of 300 to 1060 frames. The final value of the bubble departure frequency is the average between the frequencies of each nucleation site. The uncertainty associated to these measurements is ±1 fps.

Finally, the evaluation of the active nucleation sites density must be done by visual inspection of the frames, which introduces an uncertainty associated to the subjective criterion of the observer. To lessen this uncertainty, at least ten frames are chosen, at different times during the single experiment. The final values of the active nucleation site density are an average of the ten evaluated values.

2.3 PIV measurements

Several studies in the literature confirm the potential of using PIV to measure bubble velocity inside a flowing fluid, as for example reported by [8] and [9]. However, the results obtained from this technique are very sensitive to the characteristics of the flow and to the parameters used during the visualization and the post-processing of the images (*e.g.* [9]). In the present work, the main focus is to measure the velocity of the bubbles, so seeding was not used, but instead the bubbles are followed, as suggested by [9]. Bubbles diameter is in the range of 500-800 μm, measured by image post-processing. These dimensions and the low characteristic velocities of the bubbles (1-10 cm/s) require a careful analysis of all the parameters which have to be selected in the PIV configuration. The PIV system uses a CCD camera Kodak Megaplus, Model 1.0, with an image resolution of 1018x1008 pixel^2. The bubbles are illuminated via a dual Nd:YAG Litron laser. The coordinate system considered in the measurements is shown in Figure 2.

The time delay between laser pulses is varied (1<Δt<8ms) depending on the imposed heat flux: the time between pulses is smaller for higher imposed heat fluxes. Furthermore, the interrogation area and the overlap are also varied for the various imposed heat flux conditions, in an optimization process, to assure that the chosen values are adequate to obtain accurate measurements. Hence, the selected interrogation area was varied

between 16 and 64 pixels (1pixel/58μm) to assure that at least five bubbles are inside. An overlap of 50% is chosen by analyzing two consecutive frames and evaluating the average displacement of the bubbles. The most appropriate approach for this kind of flow is using a recursive cross correlation or the average correlation algorithms (*e.g.* [9]). In the present work, after analyzing extensively both approaches, the cross correlation was considered to be the most appropriate. The measurements performed using PIV are compared with extensive image post-processing, within quite good agreement. The PIV data were processed with the software Flow manager 4.2.

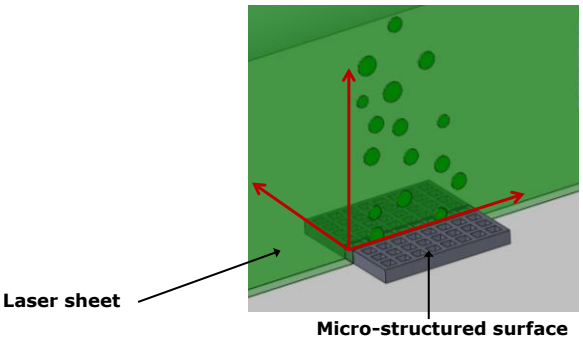

Figure 2 Coordinate system considered for the PIV measurements.

3. RESULTS AND DISCUSSION

In [4], heat transfer measurements were related to bubble dynamics to understand the effect of the micro-patterns on the heat transfer process. Mainly, the pool boiling of liquids such as water, with high latent heat of evaporation h_{fg} and high surface tension σ_{lv} was reported to be strongly affected by horizontal coalescence (the coalescence factor, as introduced in [4] $D^*=D_b/D_{nc}>>1.0$, where D_b is the averaged bubble diameter and D_{nc} is the diameter as the bubble exits the cavity, i.e. with no coalescence), which could generate large vapor blankets over the surface, which lead to a steep deterioration of the heat transfer coefficient *h*. On the other hand, for liquids with lower latent heat of evaporation and lower surface tension, the pool boiling heat transfer was suggested to be less affected by coalescence effects. Also, the evaporation parcel was speculated to be less important. However, for the fluids studied in [4], the range of h_{fg} was not wide enough to clearly confirm such trends. In this context, it is worth to perform a comparative analysis of the pool boiling of the 3 liquids used here (water, ethanol and HFE7000), covering a sufficiently wide range of thermophysical properties which are relevant for the pool boiling heat transfer mechanisms.

3.1 Effect of surface micro-patterning on bubble dynamics

Bubble dynamics of these liquids is characterized in Figure 3, which depicts the bubble departure diameter, bubble frequency and nucleation sites density, for the pool boiling of water, ethanol and HFE7000 over micro-patterned surfaces with different spacing between the cavities, *S*. The figures show that nucleation sites density naturally increases with the number of cavities (i.e. for surfaces with smaller *S*). The large value of the latent heat of evaporation of the water also delays the beginning of the boiling process, so water boiling has the lowest nucleation sites density, which increases very gradually with the heat flux and with the number of cavities (for surfaces with smaller *S*). On the other hand, the lowest value of h_{fg} of HFE7100 allows the fast activation of a large number of nucleation sites, even at low heat fluxes. The nucleation sites density then stabilizes, as the maximum number of active nucleation sites is achieved. However, this is not the main reason for improved performance of certain micro-patterned surfaces. In fact, exception made to the surface with the largest *S* (C7, S=1200μm), for which the nucleation sites density is up to 1-2 orders of magnitude smaller when compared to the other surfaces, independently of the working fluid, this is not the major parameter affected by surface micro-patterning.The analysis must be performed taking into account the mechanistic formation of the bubbles. So, considering bubble departure depends on the balance between surface tension forces ($\sim\sigma_{lv}D_b^2$) and the buoyancy forces ($\sim g(\rho_l-\rho_v)$), the largest bubbles are expected in water boiling, which is confirmed in Figure 3. This formulation has been long-established in the literature since Wark [10] and Fritz [11]. The formed bubbles also keep undetached from the surface for a long time. Under these conditions, in water pool boiling strong bubble coalescence occurs very close to the surface, where relevant heat transfer occurs. The strong coalescence of water bubbles near the wall is confirmed by the quantitative analysis of the bubble departure frequency, in Figure 3, which varies significantly with S. The lowest frequency, which is associated to a stronger effect of the interaction phenomena [4, 12] occurs for the water pool boiling. It is worth noticing that while for surfaces C2 (*S*=400μm), C5 (*S*=700μm) and C7 (*S*=1200μm), the frequency values obtained for water are quite similar to those of ethanol and HFE7000, for surface C1 (*S*=304μm), the frequency is clearly reduced for water. So, while surface C1 (*S*=304μm) allows the best bubble dynamics performance for ethanol and HFE7000, it is actually underperforming in water, when compared to surface C2 (*S*=400μm), since the distance between cavities is too small, so it is promoting an excessive coalescence.

The relation between coalescence and the distance between the cavities inferred from Figure 3 is further confirmed in Figure 4: strong coalescence effects are observed for water pool boiling (the coalescence factor $D_b/D>>1$), which are much affected by *S*. On the other hand, coalescence effects are not so strong either in ethanol or in HFE7000 (D_b/D is close to 1) and, despite D_b/D is slightly higher for surfaces with smaller *S* (more cavities), such as C1 (*S*=304μm), there is not a significantly effect of *S* in the coalescence for these liquids.

In summary, the vital role of the coalescence on the bubble dynamics, for the liquids with large σ_{lv} and h_{fg}, is proven. For these liquids the coalescence is strongly affected by the surface micro-patterning, namely by the distance between cavities (*S*). However, for liquids with small σ_{lv} and h_{fg}, the effect of the micro-patterns cannot be strictly related to coalescence phenomena.

The link between nucleation characteristics and the heat transfer is further clarified in the following subsection.

3.2 Combined effect of liquid properties and surface micro-patterning on the pool boiling heat transfer

Figure 5 depicts the boiling curves and heat transfer coefficients, as a function of wall superheat (T_w-T_{sat}) for water, ethanol and HFE7000 over the micro-patterned surfaces with varying *S*. The boiling curves highlight the best performance of water pool boiling for all the surfaces studied, which is justified by the undeniable higher values of the thermal properties of this liquid, despite the aforementioned issues related to the activation of the nucleation sites. Although ethanol and HFE 7000 presented a more homogenous and vigorous boiling with limited interaction mechanisms (and particularly coalescence), this was not enough for these fluids to reach the high heat transfer coefficients of water. Nevertheless, it is worth noticing that the strong horizontal coalescence phenomena characterizing water boiling on surface C1 (S=304 μm), lead to a steep deterioration of the heat transfer coefficient, so that the heat transfer of water and ethanol are quite similar for the aforementioned surface. Thus, structuring the surface can actually allow improving the pool boiling heat transfer, as long as one can optimize the patterns to act on the coalescence, when using liquids with high h_{fg} and σ_{lv}. In this case S is directly acting on the coalescence mechanisms which occur close to the surface and so should be related to the force balance describing the bubble detachment, as proposed by Fritz [11] and followed by many other researchers to scale bubble departure diameters: $Lc=(\sigma_{lv}/(\rho_l-\rho_v))^{1/2}$. For liquids with lower values of h_{fg} and σ_{lv}, micro-patterning leads to and improvement of the pool boiling heat transfer, but its effect must be related to other mechanisms, rather than coalescence. To infer on this, PIV measurements were performed to characterize the fluid flow and the velocity of the bubbles, as discussed in the following sub-section.

3.3 Effect of the surface micro-patterning on the fluid flow

The effect of the surface patterning on the fluid flow was investigated evaluating the average vertical bubble velocity (average of the velocity profile for a fixed value of H/D), along the vertical dimensionless distance H/D, where H is the vertical distance from the top face of the surface in (mm) and D is the bubble departure diameter (also in mm), for different heating conditions and different micro-patterns. Naturally that this effect is relevant close to the surface, but given the well known restrictions of PIV measurements performed very close to the surface (*e.g.* Raffel *et al.* [13]) the assessment of bubbles' velocity must be performed at various distances H/D, in order to understand bubbles´ motion.

The vigorous boiling activity already pointed out for HFE7000 and identified by the very high bubble frequency and nucleation sites density in Figure 3, can be also identified in the analysis of the bubbles vertical velocity profiles. There is a strong oscillation along the vertical velocity around the mean value for HFE7000, which is speculated to be due to the very vigorous boiling. Similarly to what was observed for ethanol in [4], surfaces with closer cavities (C2 S=400μm, and C5 S=700μm) present more uniform and stable profile when compared to those with sparser cavities (C6 S=800μm, and C7 S=1200μm). These results are not shown here due to paper length constrains, but they confirm the preliminary reports in [4] for the ethanol pool boiling. In fact it is now clearer that the stronger interaction phenomena still occur at the surface with closer cavities, but they are observed at a higher distance from the surface, when compared to water. Hence, the coalescence will not affect directly the heat transfer by producing vapor bubbles which block the fluid circulation near the surface, but contribute for the formation of a denser bubble plume, acting as stabilization factor when one speaks in terms of vertical velocities. A slightly difference instead can be noticed between the two fluids (HFE7000 and ethanol): for surfaces with sparser cavities, due to the high number of nucleation sites and the higher value of bubble departure frequency characterizing HFE 7000, the oscillations of the vertical velocity are more evident than those observed for ethanol. However, the vertical velocity is much higher, so overall the induced bulk convection is more efficient.

The relation between bubble velocity and wall superheat reported in Figure 6 evidences that HFE 7000 and ethanol pool boiling are both characterized by a growing vertical velocity with the wall superheat, which is an expected result given the increase of the effect of buoyancy on the bubble detachment due to the higher temperature difference between the heating surface and the liquid layer directly in contact with it. HFE 7000 is generally characterized by higher vertical velocities, when compared to ethanol, which is attributed to lower surface tension (giving rise to smaller bubbles) and high liquid density (thus the buoyancy forces are larger). This is more significant for surfaces with smaller *S* thus suggesting that for liquids with smaller surface tension and smaller latent heat of evaporation, the distance between the cavities *S* is associated to the flow (and to the characteristic velocity) thus its main role will be to improve the bulk induced convection. Even though the heat transfer by enhanced bulk convection is more effective in HFE7000, the extremely low value of the latent heat of evaporation is not enough to overcome the larger absolute value of the evaporative parcel of ethanol. Hence Figure 7 which gives the relation of the overall mean values of h with the vertical velocity does not allow to detect the good performance of HFE7000.

On the other hand, the alternative representation suggested in Figure 8, already allows to understand the relative improvement of the performances using the micro-patterned surfaces since, on one hand compares the enhancement of the heat transfer coefficient (given by the three heat transfer parcels: natural convection, evaporation and induced bulk convection) using each micro-textured surface in relation to that of the smooth surface. On the other hand, the distance *S* is related to the characteristic bubble departure dimensions. This relation is important as it defines the critical distance *S* up to which the bubbles with a certain diameter, depending on the balance between surface tension and buoyancy forces ($Lc=(\sigma_{lv}/(\rho_l-\rho_v))^{1/2}$) will coalesce. Such relation must still be refined, but one may already identify a maximum for the water boiling, which is related to the maximum *S* above which the horizontal coalescence will conduce to the declination of the heat transfer coefficient (as identified in the boiling curves in Figure 5).

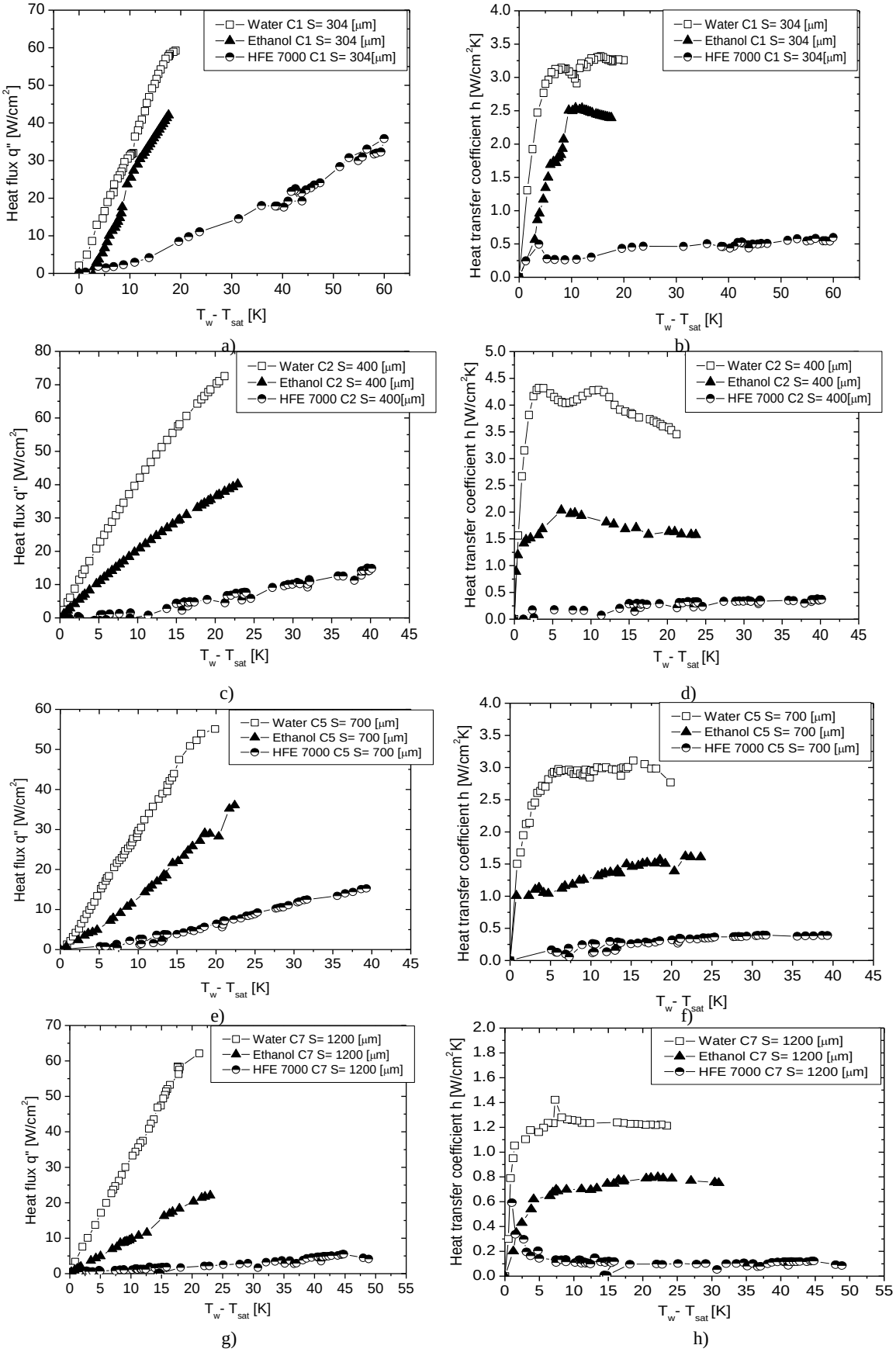

Figure 5 Boiling curves and heat transfer coefficients for Water, ethanol and HFE7000 boiling over: a), b) Surface (C1 S=304 μm); c),d) Surface C2 (S=400 μm) e),f) Surface C5 (S=700) g),h) Surface C7 (S=1200).

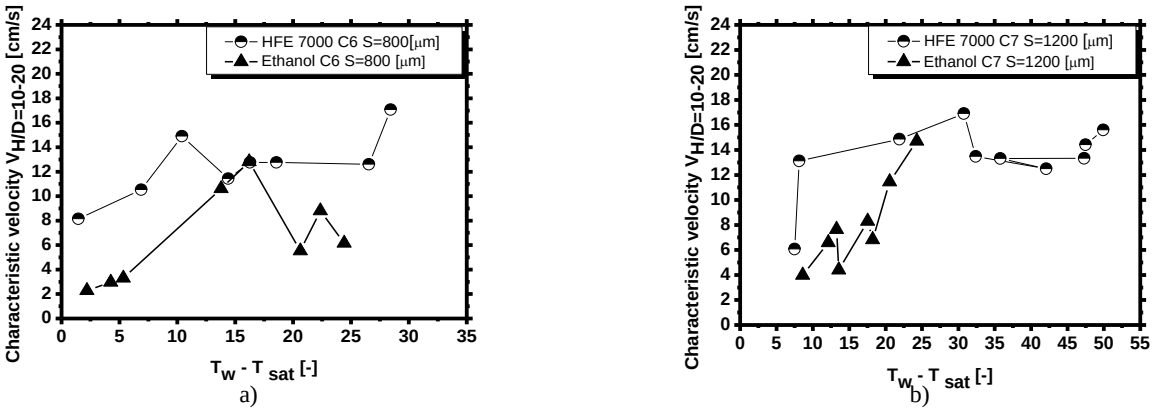

Figure 6 Characteristic velocity vs wall superheat for HFE 700 and ethanol. a) Surface C2 (S=400 μm) b) Surface (C5 S=700 μm9 c) Surface (C6 S=800 μm) d) Surface (C7 S=1200 μm).

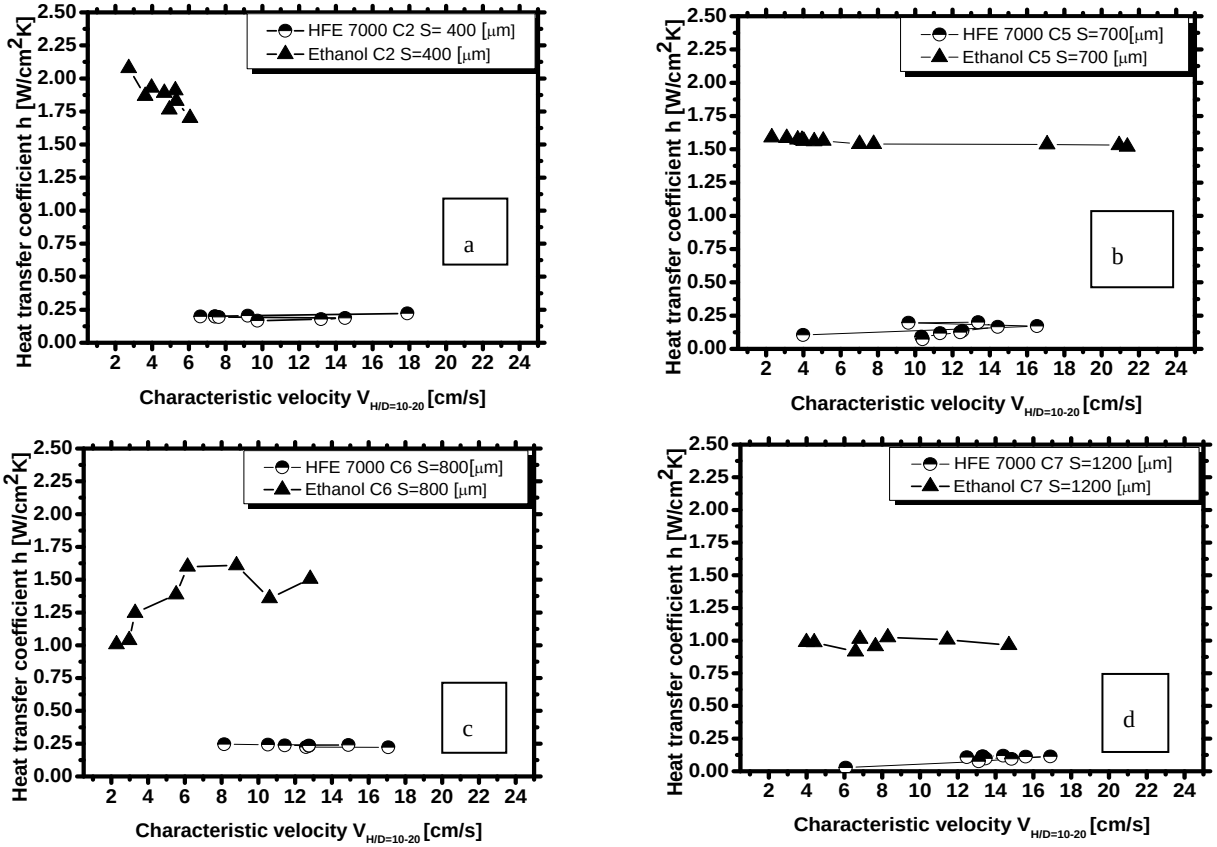

Figure 7 Heat transfer coefficient versus characteristic velocity for HFE 700 and ethanol. a) Surface C2 (S=400 μm), b) Surface C5 (S=700 μm), c) Surface C6 (S=800 μm), d) Surface C7 (S=1200 μm).

The absolute values of h, being the result of the sum of the 3 parcels of the heat transfer [6] are dominated by the largest values of the latent heat of evaporation which occur for the water. However, the plot in Figure 8 clearly indicates that although the latent heat of evaporation of ethanol is yet significantly larger than that of HFE7000, the relative enhancement in the heat transfer obtained with the micro-patterned surfaces is higher than that obtained for ethanol, so the curve for HFE700 is above that of ethanol.

Reminding that the pool boiling heat transfer results from the sum of 3 parcels:

q=natural convection+evaporation+induced bulk convection , the large heat transfer coefficients associated to the water pool boiling are perfectly understandable, given the well know larger order of magnitude of the evaporative parcel in comparison to the natural convection (e.g. [14]). The strong coalescence factor may also mitigate the induced bulk convection, so, from the phenomenological point of view, *S* is well related to the characteristic length ($Lc=(\sigma_{lv}/(\rho_l-\rho_v))^{1/2}$). For liquids with lower values of h_{fg}, the analysis presented above suggests a dominant role of the induced bulk convection. The relative importance of each parcel was investigated in the present study. The results cannot be depicted in this paper, due to length constrains, but

confirm the dominance of the parcel of the induced bulk convection. Hence, *S* must be related to the flow (*e.g.* to the characteristic velocity) in order to fully describe the effect of *S* in the heat transfer. This task is a non-trivial work in progress, which requires further investigation. However, the first step is completed: the effect of *S* in each of the heat transfer parcels was identified, thanks to the combined analysis of the heat transfer with the boiling dynamics. This analysis was performed covering a sufficiently wide range of liquid properties, for which the predominant parcel of the heat transfer is different. This procedure allows to focus on each parcel.

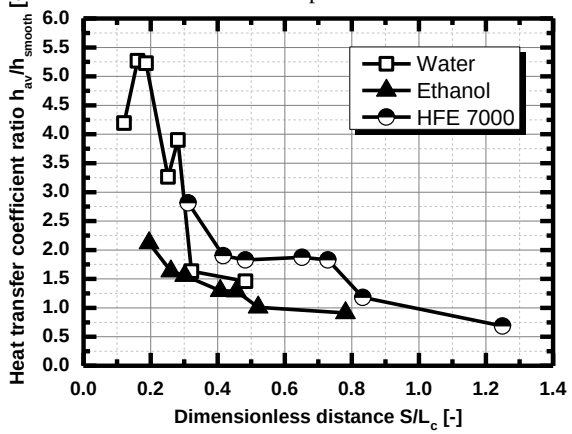

Figure 8 Heat transfer ratio vs dimensionless distance for water, ethanol and HFE 7000 in the range of patterns studied.

FINAL REMARKS

The present paper addresses a detailed analysis which combines heat transfer measurements with the description of the boiling mechanisms to describe the effect of using micro-patterned surfaces on the pool boiling heat transfer. The micro-patterns are composed by arrays of cavities with fixed shape and depth, only varying the distance between cavities, *S*. High-speed visualization and image post-processing were used to quantify the nucleate boiling characteristics. Additionally, the effect of the surface patterning on the fluid flow was investigated evaluating the average vertical bubble velocity by PIV measurements. Pool boiling heat transfer is a sum of three parcels: natural convection, evaporation and bulk induced convections. The results indicate that *S* plays a different role in each of these parcels. Thus, for liquids with high values of surface tension and latent heat of evaporation, the evaporative parcel is of major importance. For these liquids there is a strong coalescence effect near the surface which may lead to a fast decline of the heat transfer coefficient due to the formation of large vapor bubbles, and to the mitigation of the parcel of the induced bulk convection. In this case, *S* must be used to control the coalescence effect. On the other hand, for liquids with small surface tension and latent heat of evaporation, the coalescence is much less evident and does not occur so close to the surface. The experimental results suggest a dominant role of the induced bulk convection parcel, which was theoretically confirmed. In this case *S* will act on the flow stabilization and on the characteristic vertical bubble velocity.

ACKNOWLEDGEMENTS

The authors are grateful to Fundação para a Ciência e a Tecnologia (FCT) for partially financing the research under the framework of project PTDC/EME-MFE/109933/2009 and for supporting A.S. Moita with a Fellowship (Ref.:SFRH/BPD/63788/2009).

REFERENCES

1. K-H Chu, R. Enright R and E.N.Wang "Structured surfaces for enhance pool boiling heat transfer" Appl. Phys. Lett. 100, 241603, 2012.
2. S. Fischer, E. M. Slomski, P. Stephan, M. Oechsner "Enhancement of nucleate boiling heat transfer by micro-structured chromium nitride surfaces" Journal of Physics: Conf. Series 395, 012128 (doi:10.1088/1742-6596/395/1/012128), 2012.
3. J.P. McHale and S.V. Garimella "Bubble nucleation characteristics in pool boiling of wetting liquid on smooth and rough surfaces" Int. J. Multiphase Flow 35, pp.249-260, 2010.
4. A.S. Moita, E. Teodori E and A.L.N. Moreira "Enhancement of pool boiling heat transfer by surface micro-structuring" J. Physics: Conf. Series 395, 012175 (doi: 10.1088/1742-6596/395/1/012175), 2012.
5. A.S. Moita, A.L.N. Moreira "Scaling the effects of surface topography in the secondary atomization resulting from droplet/wall interactions" Exp. Fluids 52(3), pp.679-695, 2012.
6. C.Y. Han and P. Griffith "The mechanism of heat transfer in nucleate boiling" Technical Report No 7673-19, Dep. Mech. Eng. MIT, USA, 1992.
7. H. Bostanci "Thermal Challenges in Next Generation Electronic Systems" Joshi & Garimella (Eds), Millpress, Rotterdam, ISBN 90-77017-03-8 (2002).
8. T. Sasaki, N. Nagai, Y. Murai, F. Yamamoto, "Particle Image Velocimetry measurement of bubbly flow induced by alkaline water electrolysis" In: Proc. of PSFVIP-4, Chamonix, France (2003).
9. W. Cheng, Y. Murai, T. Sasaki, F. Yamamoto "Bubble velocity measurement with a recursive cross correlation PIV technique" Flow Meas. Instr 16, pp.35-46, 2005.
10. W. Wark, "The Physiscal Chemistry of Flotation", I, J Phys. Cherm. 3 7:623-644 (1933)
11. W.Fritz, "Maximum Volume of Vapor Bubbles" Phys Z.36:279-385 (1935)
12. L. Zhang, M. Shodji "Nucleation sites interaction in pool boiling on the artificial surface" Int. J Heat Mass Transf., 46(3), pp.513-522, 2003.
13. M. Raffel, C. Willert, S. Wereley, S., Kompenhans, Particle Image Velocimetry: a practical guide. 2nd Ed., Springer Verlag, Heidelberg (2007).
14. F.P. Incropera, D.P DeWitt, *Fundamentals of Heat and Mass Transfer*, 3rd Ed., Wiley, 1995.